Electronic Supplementary Information

Experiment Section

Materials

Most of the reagents are from Maclin Biochemical Technology Co., Ltd. (Shanghai, China), including ammonium fluoride (NH_4F), ferric nitrate nonahydrate ($Fe(NO_3)_3{\cdot}9H_2O$), ethylenediaminetetraacetic acid disodium ($C_{10}H_{14}N_2Na_2O_8$), sodium hydroxide (NaOH), potassium phosphate monobasic (KH_2PO_4), N, N-diethyl-p-phenylenediamine (DPD), sodium hypophosphite (NaH_2PO_2), urea, disodium phosphate anhydrous (Na_2HPO_4), and nickel nitrate hexahydrate ($Ni(NO_3)_2{\cdot}6H_2O$). From Beijing Chemical Reagent Co., Ltd., we bought ethanol and hydrochloric acid (HCl). Potassium hydroxide (KOH), Nafion (5 wt%), ruthenium oxide (RuO_2), sodium chloride (NaCl), vanadium trichloride (VCl_3), sodium carbonate anhydrous (Na_2CO_3), and Pt/C (20 wt% Pt) were all acquired from Shanghai Aladdin Co., Ltd. Before usage, the maximum amount of calcium and magnesium salts is removed from Qingdao's natural seawater in Shandong Province, China. To achieve this, 6.8 g of Na_2CO_3 was added to 1 L of natural seawater, and the precipitate was filtered out before use. The supplier of the Ni foam (NF) utilized in the research was Xingtai's Qingyuan Metal Materials Co., Ltd. A Millipore system was used to purify the ultrapure (UP) water used in the experiments. No further purification was necessary because the chemical was used as supplied.

Synthesis of V_2O_3/NiFeP/NF and NiFeP/NF

First, NF (2 × 3 cm^2) was subjected to ultrasonic cleaning in 3 M HCl, UP water, and ethanol for 15 min each. Next, 15 mM $Ni(NO_3)_2$ $6H_2O$, 2.5 mM $Fe(NO_3)_3$ $9H_2O$, 2.5 mM VCl_3, and 45 mM urea were dissolved in a mixed solution of distilled water (65 mL) and ethanol (15 mL) under stirring conditions to form a clear solution. Then, the above mixture solution (35 mL and NF) was placed in a 50 mL Teflon-lined autoclave. The autoclave was maintained at 160 °C for 12 h. Obtaining NiFeV LDH/NF; if VCl_3 is not added, NiFe LDH/NF is obtained. Two ceramic boats were placed with a piece of NiFeV LDH/NF and 1 g of NaH_2PO_2 powder, respectively, with the latter at the tube furnace's upstream side. The device was heated to 300 °C at 2 °C/min in an Ar atmosphere and held at this temperature for 2 h (the same process used for NiFe LDH/NF yielded NiFeP/NF).

Preparation of RuO_2/NF and Pt/C/NF

5 mg RuO_2 was added into a solution containing 30 μL of Nafion, 485 μL of ethanol, and 485 μL of ultrapure water with the aid of ultrasonication (30 min) to form a homogeneous ink (5 mg mL^{-1}). 300 μL of catalyst ink was dropped onto a piece of cleaned NF (0.5 × 0.5 cm^2) with a loading mass of 1.5 mg cm^{-2}. Except RuO_2 is replaced by Pt/C, the remaining experimental scheme is the same as that of RuO_2/NF.

Characterization

XRD data were acquired on a Philip D8 diffractometer and a Cu Ka radiation source. SEM images were collected on a Gemini SEM 300 scanning electron microscope (ZEISS, Germany) at an accelerating voltage of 5 kV. TEM images were taken on a Jem-2100F electron microscope operated at 200 kV. XPS measurements were performed on an ESCALAB 250 Xi Quantitative Scanning Microprobe. Raman spectroscopy was recorded on the Lab RAM HR Evolution confocal microscope with a source length of 532 nm.

Electrochemical test

OER experiments were performed with the CHI 660E electrochemical workstation, using the prepared samples (0.5 × 0.5 cm^2), carbon rod, and Hg/HgO as the working electrode, counter electrode, and reference electrode, respectively. Linear scanning voltammetry (LSV) curves were recorded from 0 to 1.3 V at a scan rate of 5 mV s^{-1}, with the OER scan mode set to back sweep except for Fig. S17. The pH values of 1 M KOH, 1 M KOH + 0.5 M NaCl, and 1 M KOH + seawater electrolytes are approximately 14. Electrochemical impedance spectroscopy tests were conducted across a frequency range from 2×10^5 to 0.01 Hz with amplitude of 1 mV in 1 M KOH seawater. All measured potentials were referenced to that of RHE ($E_{RHE} = E_{Hg/HgO} + 0.098\ V + 0.059 \times pH$).

Determination of active chlorine

The concentration of active chlorine in the electrolyte was determined using a UV-vis spectrophotometer in conjunction with the DPD colorimetric method (J. G. Vos and M. T. M. Koper, *J. Electroanal. Chem.*, 2018, **819**, 260–268). To initiate the analysis, 100 μL of the electrolyte, which had undergone a long-term stability test at 1000 mA cm^{-2}, was sequentially mixed with 50 μL of 1.0 M H_2SO_4, 50 μL of 2.0 M NaOH, and 4.8 mL of deionized water. Subsequently, 250 μL of DPD reagent and 250 μL of PBS (pH 6.5) were added to the solution, resulting in the development of a pink color. The active chlorine concentrations were analyzed through UV-vis absorption spectrometry at 550 nm.

Fabrication of AEM electrolyzer

The AEM was comprised of a cathode and an anode with a geometric area of 1 cm^2. The prepared electrodes of V_2O_3/NiFeP/NF and Pt/C/NF were selected as OER and HER electrodes, respectively. The cell was fed with 1 M KOH + seawater flowing at a fixed velocity of 50 mL min^{-1}. The full-cell performance was carried out at room temperature, and the data was recorded on the CHI 660E analyzer.

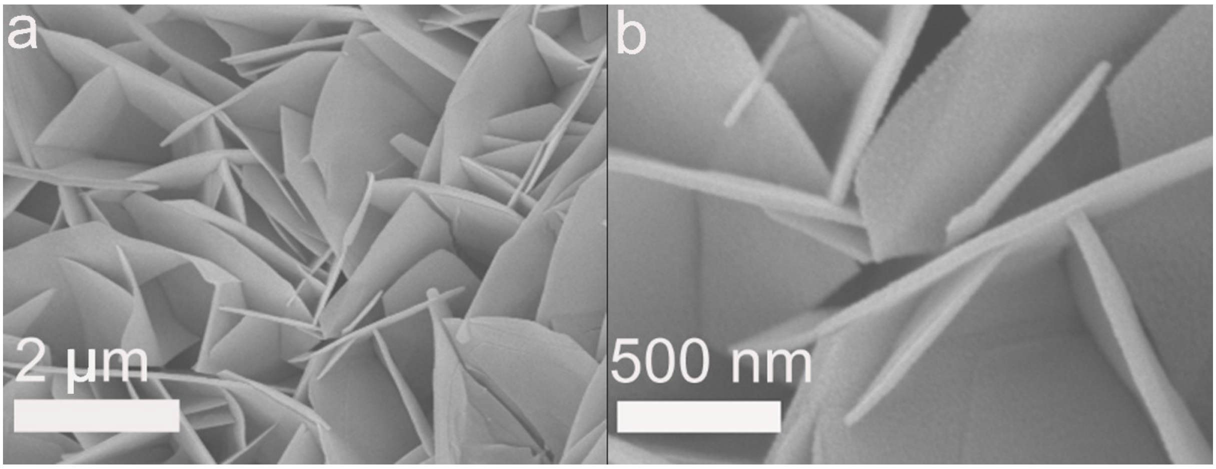

Fig. S1. (a) Low- and (b) high-magnification SEM images of NiFeP/NF.

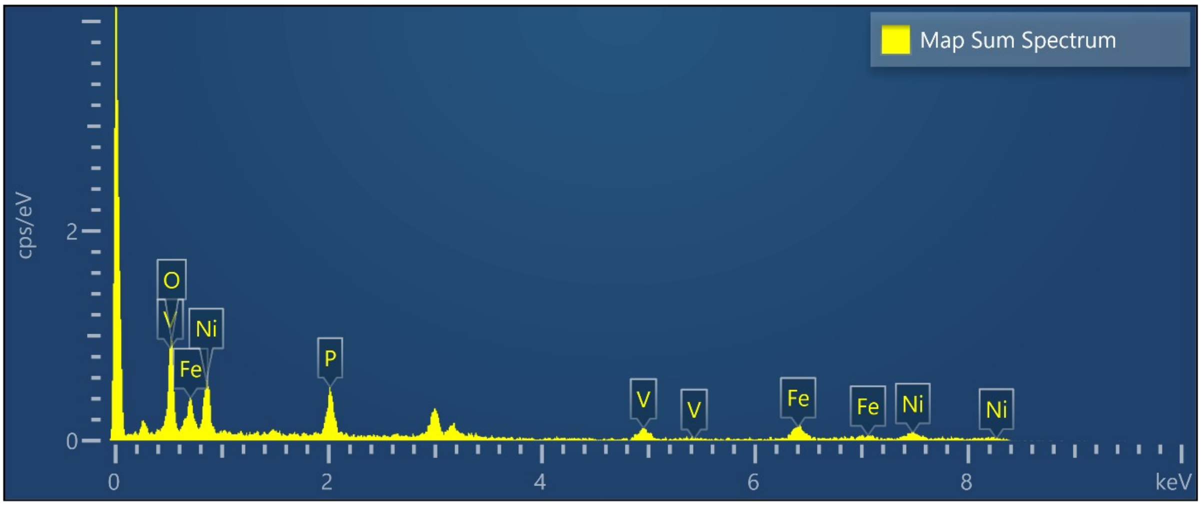

Fig. S2. EDX spectrum of V_2O_3/NiFeP/NF.

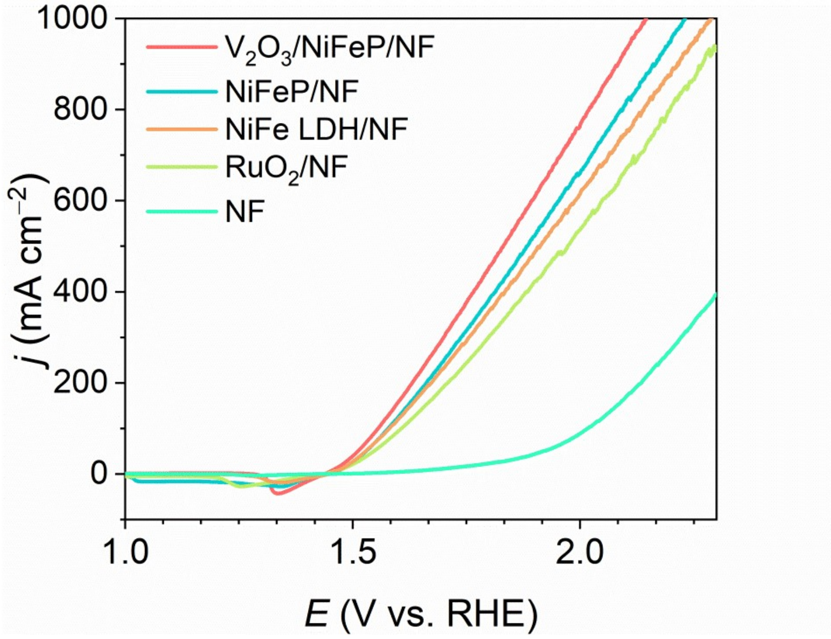

Fig. S3. LSV curves of different catalysts without iR compensation in 1 M KOH + seawater.

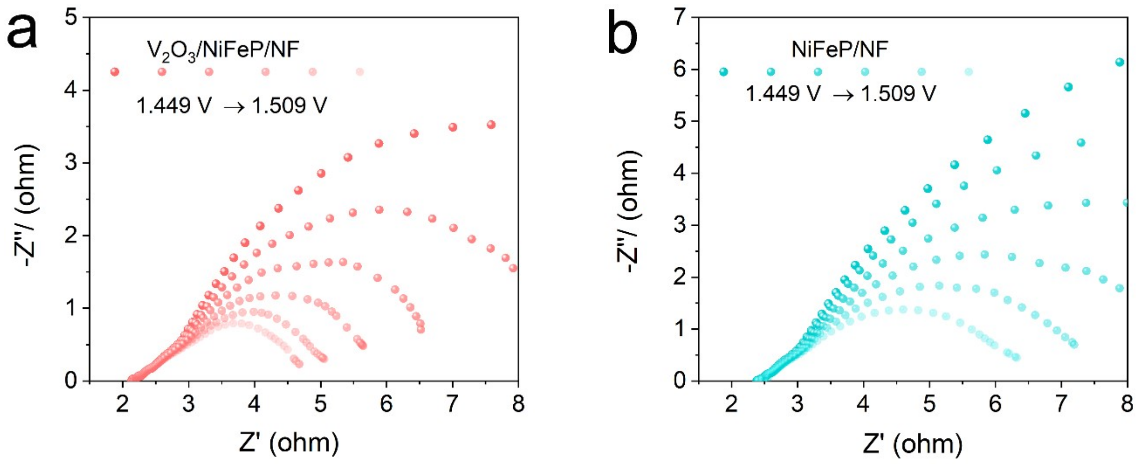

Fig. S4. Nyquist plots of (a) V_2O_3/NiFeP/NF and (b) NiFeP/NF at different potentials (vs. RHE) for OER.

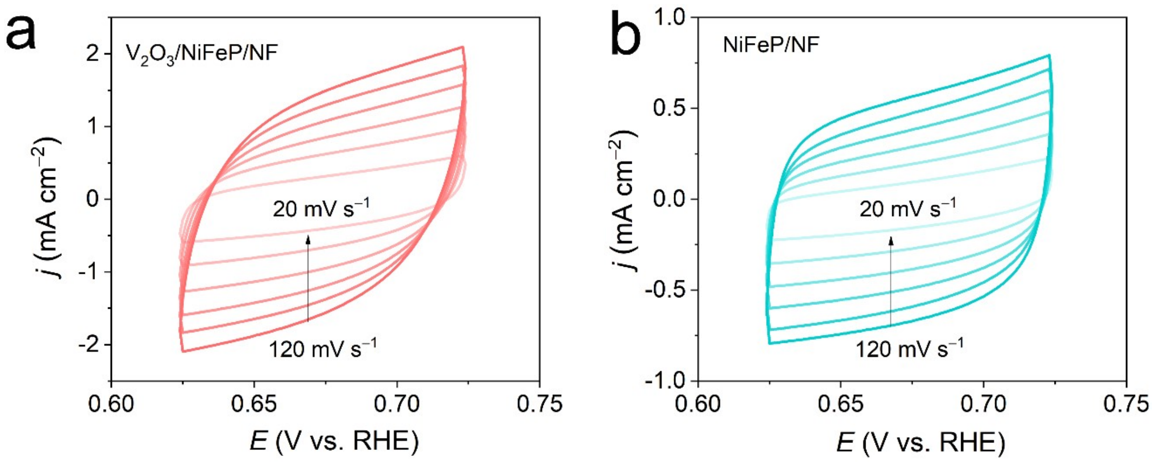

Fig. S5. CV curves of (a) V_2O_3/NiFeP/NF and (b) NiFeP/NF in the double layer region at different scan rates of 20, 40, 60, 80, 100, and 120 mV s^{-1} in 1 M KOH + seawater.

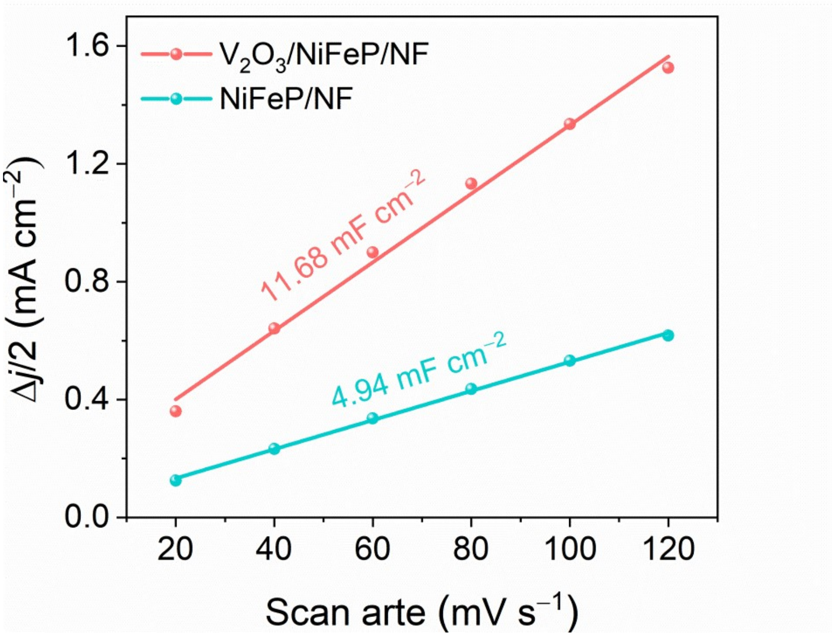

Fig. S6. C_{dl} curves of V_2O_3/NiFeP/NF and NiFeP/NF for OER.

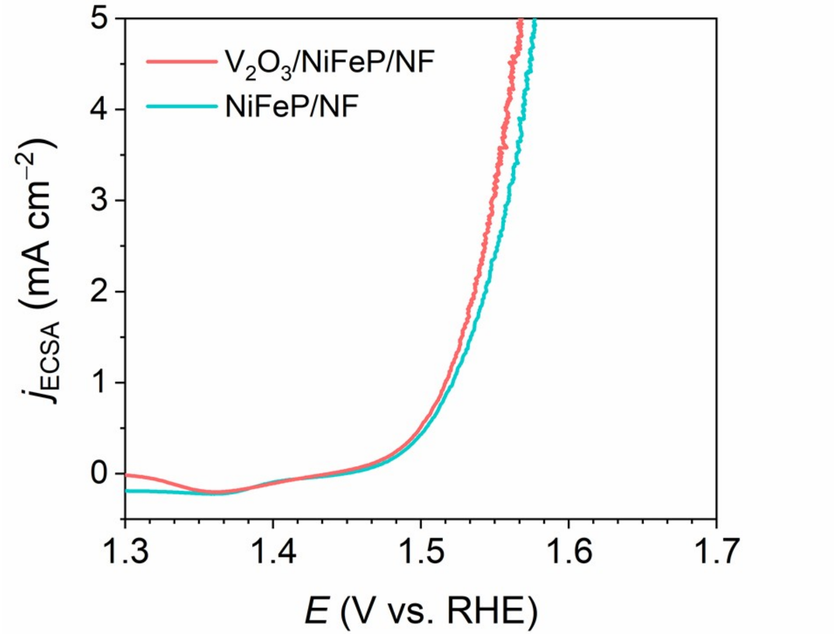

Fig. S7. LSV curves for V_2O_3/NiFeP/NF and NiFeP/NF normalized by the electrochemical active surface area in 1 M KOH + seawater.

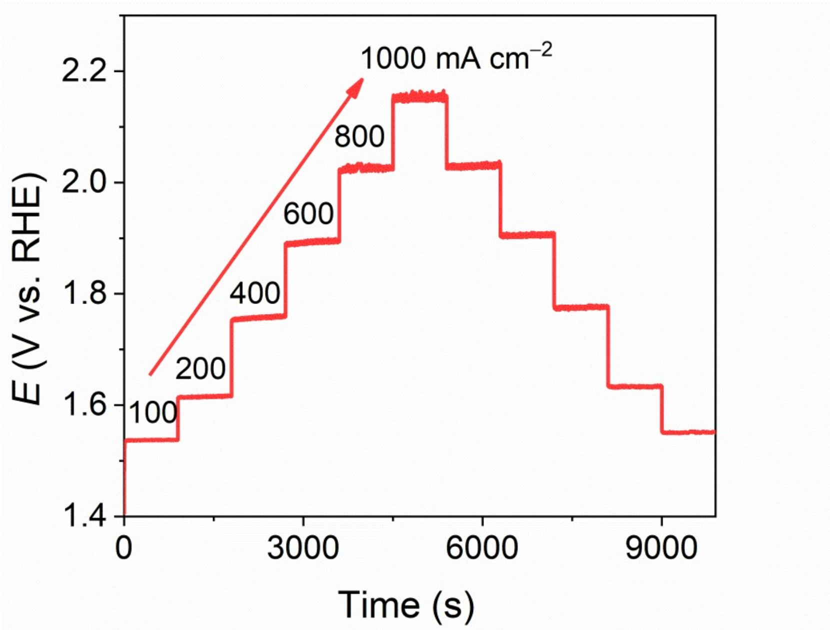

Fig. S8. Multistep chronopotentiometric curve of V_2O_3/NiFeP/NF without iR correction in 1 M KOH + seawater.

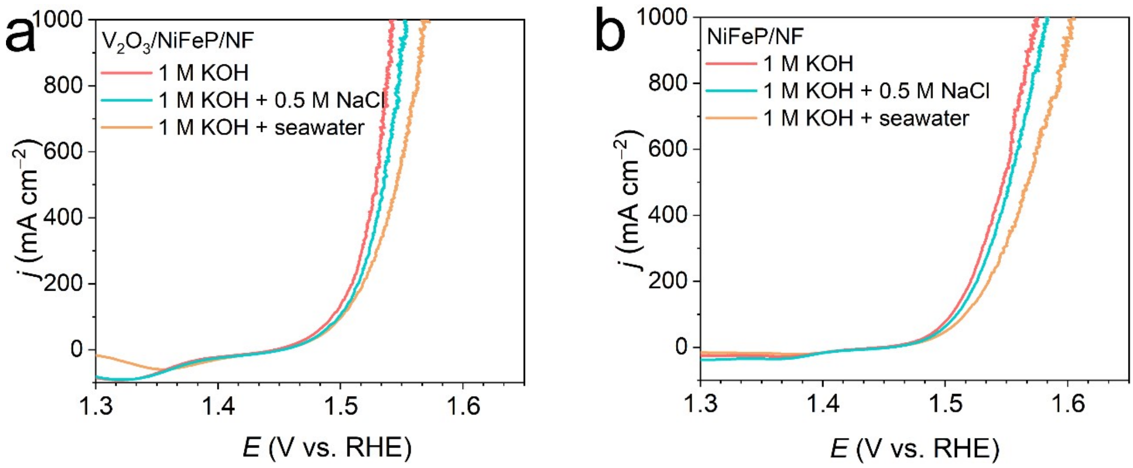

Fig. S9. LSV curves of V_2O_3/NiFeP/NF and NiFeP/NF in different electrolytes.

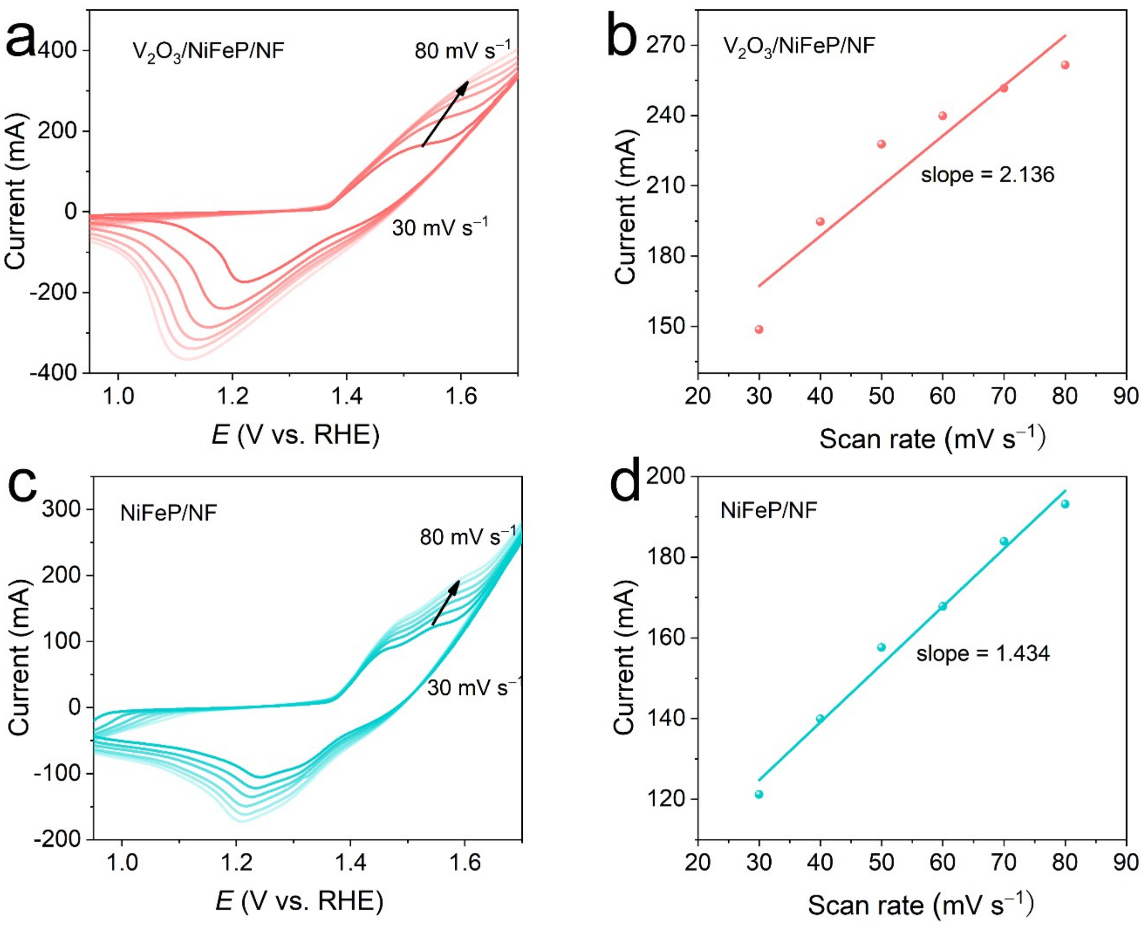

Fig. S10. CV curves for (a) V_2O_3/NiFeP/NF and (c) NiFeP/NF at different scan rates increasing from 30 to 80 mV s^{-1} in 1 M KOH + seawater. Oxidation peak current versus the scan rate plots for (b) V_2O_3/NiFeP/NF and (d) NiFeP/NF.

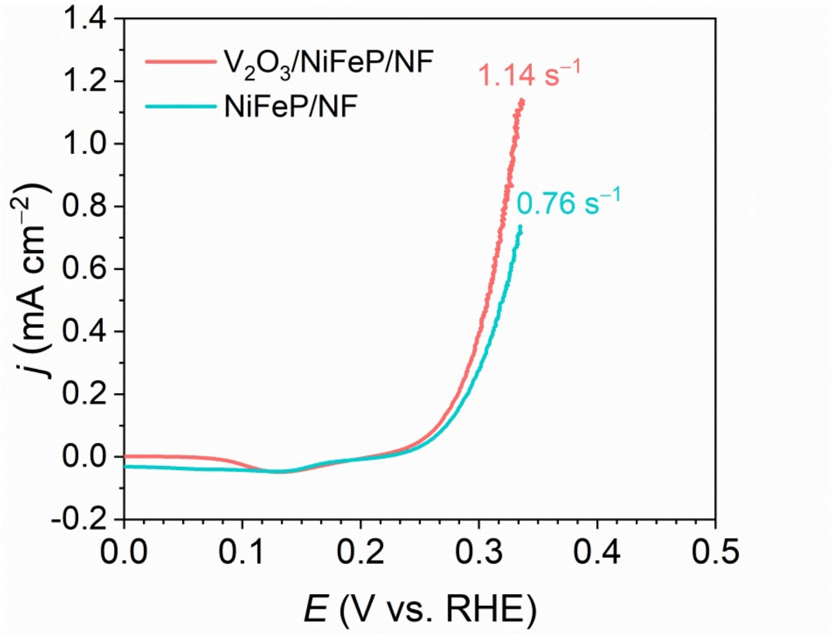

Fig. S11. TOF plots of V_2O_3/NiFeP/NF and NiFeP/NF.

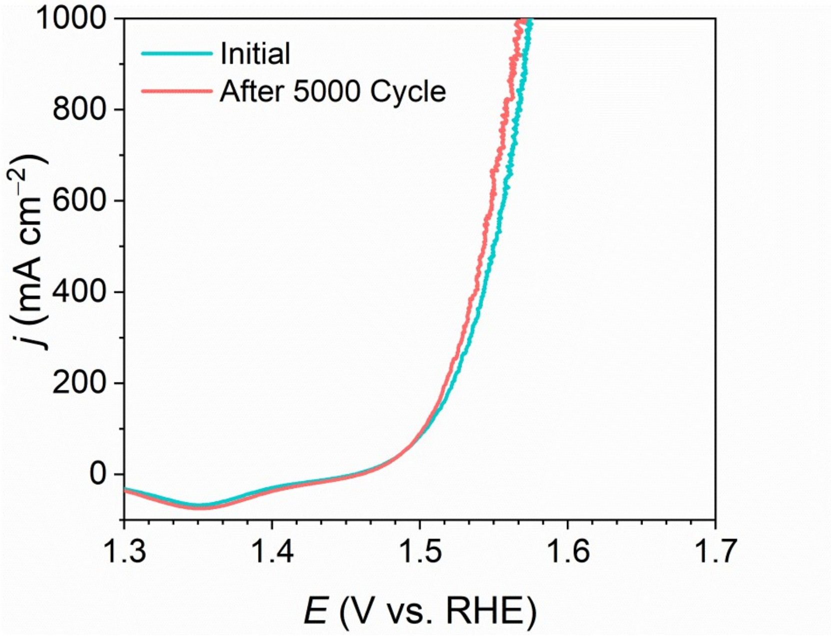

Fig. S12. LSV curves of V_2O_3/NiFeP/NF before and after 5000 CV cycles in 1 M KOH + seawater.

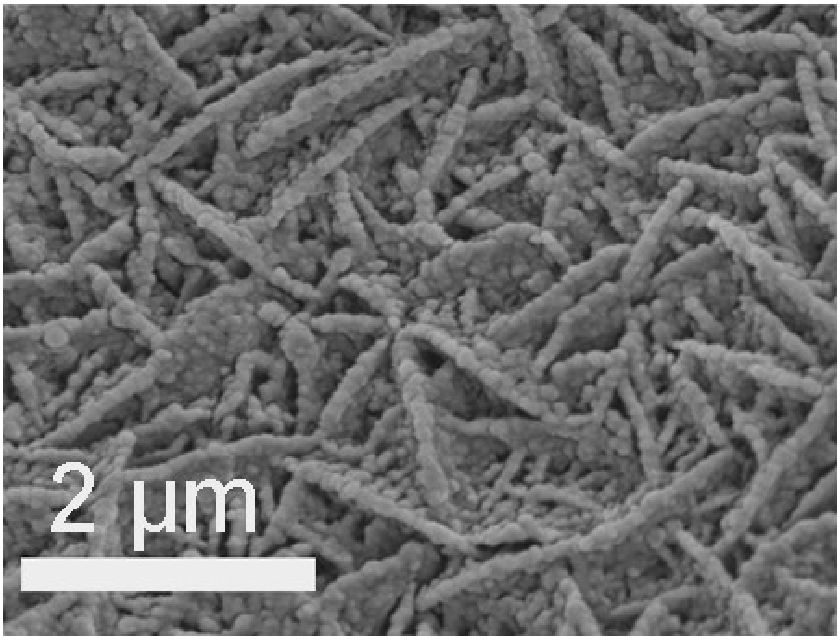

Fig. S13. SEM image of V_2O_3/NiFeP/NF after stability test in 1 M KOH + seawater.

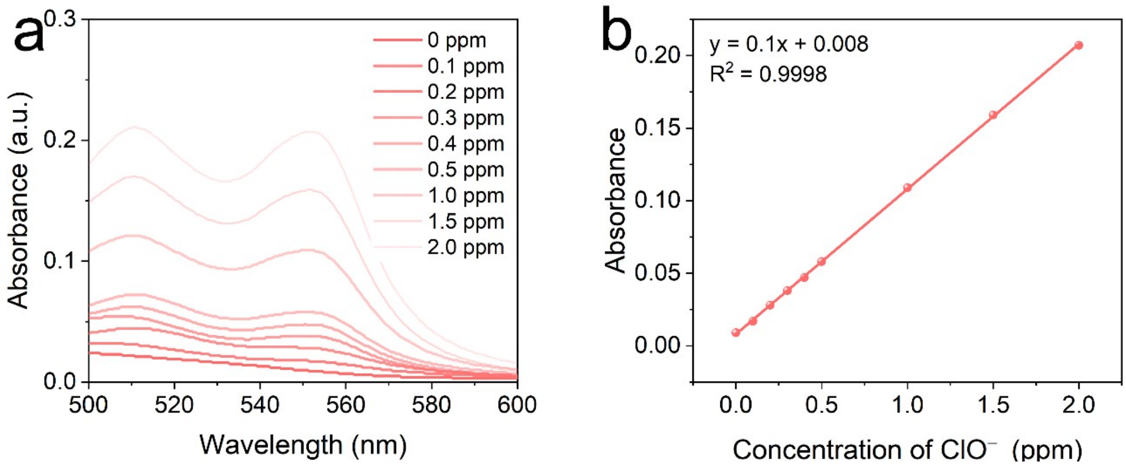

Fig. S14. (a) UV-vis absorption spectra of various active chlorine concentrations and (b) corresponding linear fit.

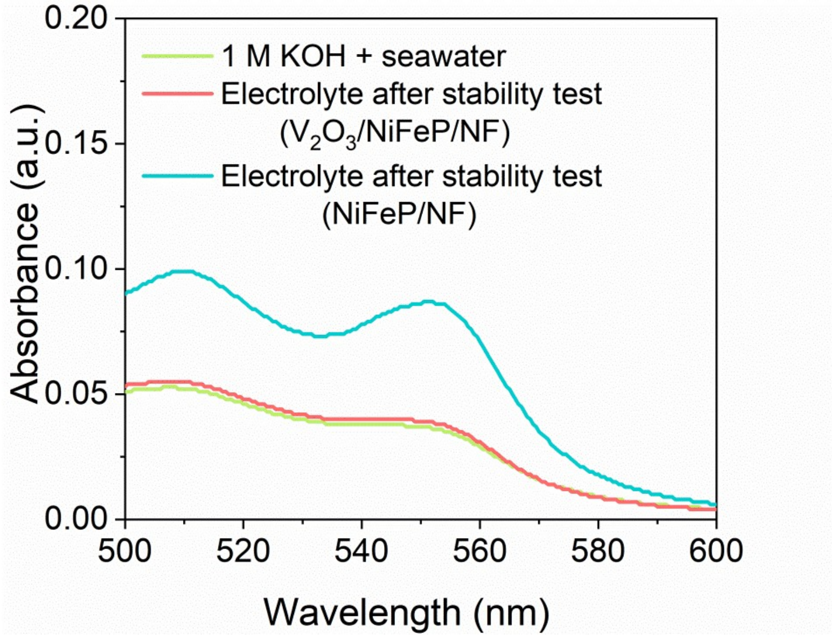

Fig. S15. UV-vis absorption spectra of electrolytes after the stability test.

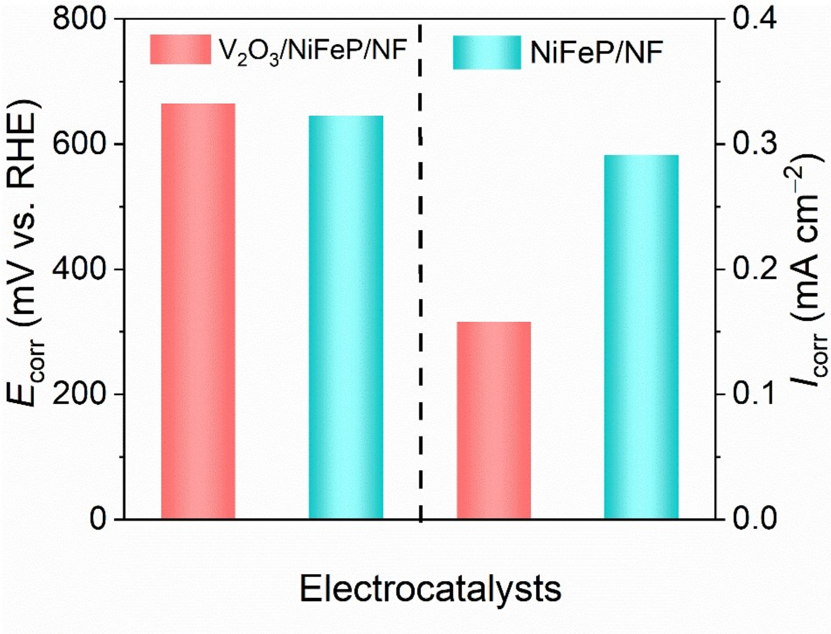

Fig. S16. Corresponding E_{corr} and I_{corr} of V_2O_3/NiFeP/NF, and NiFeP/NF in 1 M KOH + seawater.

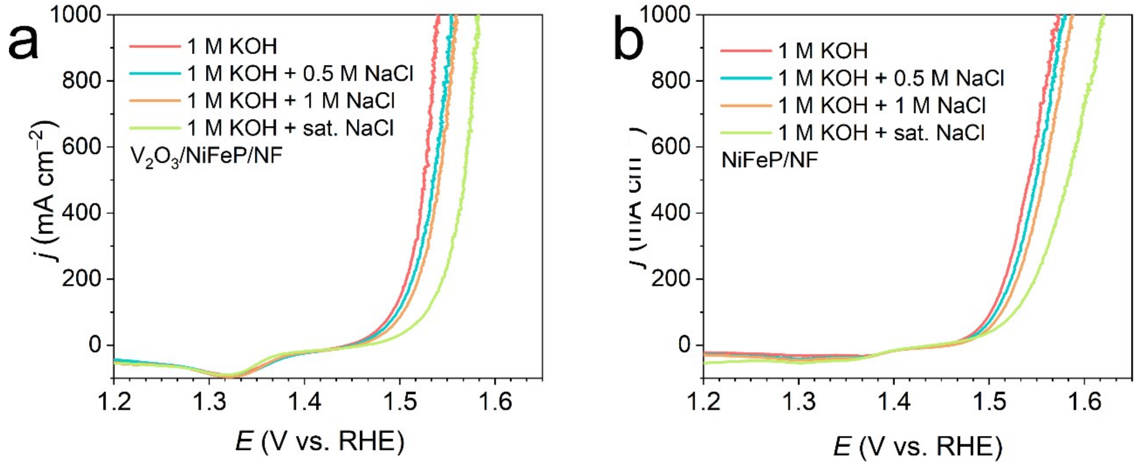

Fig. S17. LSV curves of (a) V_2O_3/NiFeP/NF and (b) NiFeP/NF in 1 M KOH + x M NaCl (x = 0, 0.5, 1.0, and saturated)

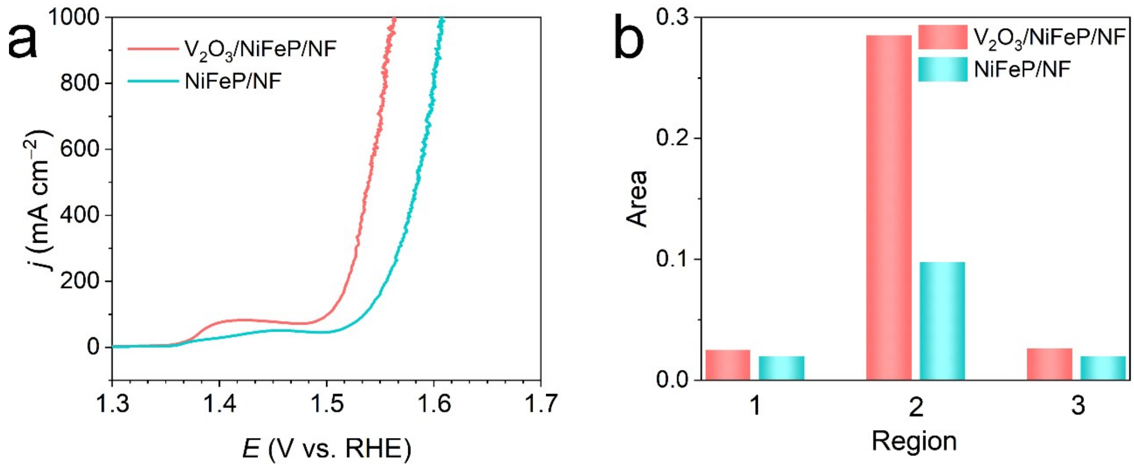

Fig. S18. (a) FTacV corresponding to LSV curves of V_2O_3/NiFeP/NF and NiFeP/NF. (b) corresponding region integral area.

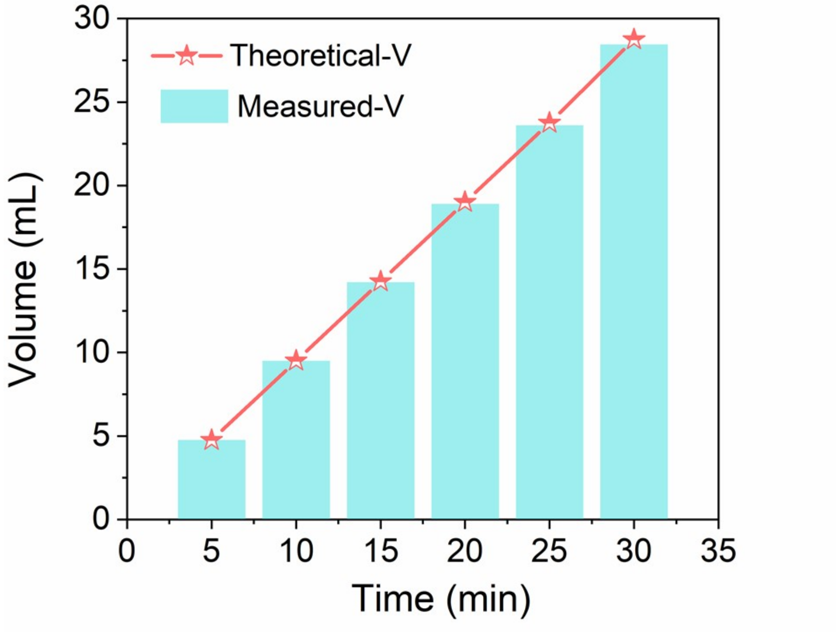

Fig. S19. Comparison between the amount collected experimentally and calculated O_2 for V_2O_3/NiFeP/NF theoretically at a *j* of 1 A cm^{-2} in 1 M KOH + seawater with three independent replicates.

Table S1. Ion compositions of the natural seawater (before the seawater alkalization) and alkaline seawater (after the seawater alkalization) used in this work.

Species	Conc. [mg L^{-1}] for natural seawater	Conc. [mg L^{-1}] for alkaline seawater
Mg^{2+}	751.24	0.63
Ca^{2+}	269.52	9.27

Notes: The seawater was collected from Huangdao district, Qingdao city, China. The pH value for natural seawater was around 7.95, and pH for alkaline seawater was around 14.00.

Table S2. The results of electrochemical impedance (R_s) and resistivity (ρ).

Sample	NiFeP/NF	V_2O_3/NiFeP/NF
$\mathbf{R_s}$	2.422	2.142
ρ	30.275	26.775

Table S3. Comparison of the OER performance of V_2O_3/NiFeP/NF with reported ASO electrocatalysts.

Electrodes	Electrolyte	Overpotential (mV)/mA cm^{-2}	Stability (h)/mA cm^{-2}	Ref.
V_2O_3/NiFeP/NF	**1 M KOH + seawater**	**267/100 311/500 335/1000**	**1000/1000**	**This work**
Ni_2P@$NiMoO_4$/NF	1 M KOH + seawater	292/100 343/500 370/1000	500/1000	*Small*, 2024, **20**, 2400141
Mn-doped Ni_2P/Fe_2P	1 M KOH + seawater	270/100 325/500 358/1000	200/500 200/100	*Chem. Eng. J.*, 2023, **454**, 140061
Ni_3S_2/Fe-NiP_X/NF	1 M KOH + seawater	336/500 351/1000	100/0.1 100/0.5	*Adv. Sci.*, 2022, **9**, 2104846
NiFeP/NF	1 M KOH + seawater	328/500 370/1000	100/100	*Inorg. Chem.*, 2024, **63**, 20792−20801
Mn-FeP_V/IF	1 M KOH + seawater	376/500 395/1000	45/100	*Small*, 2024, **20**, 2308613
NiIr-LDH/NF	1 M KOH + seawater	315/100 361/1000	650/500	*J. Am. Chem. Soc.*, 2022, **144**, 9254−9263
F-$FeCoP_V$@IF	1 M KOH + seawater	280/100 340/1000	20/100	*Appl. Catal. B: Environ.*, 2023, **328**, 122487
FeMo-NiP_X/NF	1 M KOH + seawater	273/100 326/500 359/1000	150/1000	*Inorg. Chem. Front.*, 2024, **11**, 498−507
RuNi-Fe_2O_3/IF	1 M KOH + seawater	329/100 387/500 424/1000	20/100	*Chin. J. Catal.*, 2022, **43**, 2202–2211
Fe-NiO/MoO_2	1 M KOH + seawater	270/100 338/500 399/1000	/	*Nano Energy*, 2024, **128**, 109921
Ru-FeP_4/IF	1 M KOH + seawater	370/100 470/1000	20/100	*Appl. Catal. B: Environ.*, 2022, **319**, 121950
NiFe LDH-CeW@NFF	1 M KOH + seawater	330/500 387/1000	100/1000	*Appl. Catal. B: Environ.*, 2023, **330**, 122612

CD_S-Mn-Co_XP	1 M KOH + seawater	420/500 470/1000	100/500	*Small*, 2024, **20**, 2402478